Available online at www.sciencedirect.com
ScienceDirect
Journal of Catalysis 251 (2007) 338–344
JOURNAL OF CATALYSIS
www.elsevier.com/locate/jcat

Dramatic liquid-phase dehydrogenation rate enhancements using gas-phase hydrogen acceptors

K.T. Hindle [a], R. Burch [a], P. Crawford [a], C. Hardacre [a,*], P. Hu [a], B. Kalirai [b], D.W. Rooney [a]

[a] *CenTACat, School of Chemistry and Chemical Engineering, Queen's University, Belfast, BT9 5AG, UK*
[b] *Robinson Brothers Ltd., Phoenix Street, West Bromwich, B70 0AH, UK*

Received 13 June 2007; revised 25 July 2007; accepted 27 July 2007

Available online 14 September 2007

Abstract

The dehydrogenation of 1,2,3,4-tetrahydrocarbazole (THCZ) to form carbazole (CZ) over supported palladium catalysts was examined in the presence of hydrogen acceptors. As expected, liquid hydrogen acceptors increased the rate of reaction but, importantly, gaseous hydrogen acceptors also have been used. Ethene, propene, and but-1-ene showed up to a fivefold increase in the rate of dehydrogenation. Moreover, compared with the analogous liquid systems, the gaseous alternatives are a potentially more economic method of enhancing the activity and provide a simpler workup. The mechanism for the increase in rate was examined by density functional theory calculations, which showed that the propene hydrogenation competes effectively with the back-hydrogenation of the intermediates formed during the THCZ dehydrogenation, resulting in a shift in the equilibrium toward to the formation of CZ.

Keywords: Dehydrogenation; Palladium; Carbazole; Tetrahydrocarbazole; Hydrogen acceptor; Tetrahydronaphthalene; Naphthalene; DFT

1. Introduction

Carbazole (dibenzopyrrole) and pyridocarbazole are well-known pharmacophores present in many biologically active compounds [1,2], carbazole alkaloids exhibit various biological activities, including antitumor, antibacterial, antimicrobial, and anti-inflammatory [3–5]. Carbazole is also an important building block in the synthesis of substituted carbazoles for optical applications where the functionalisation provides the photorefractive, electrical, and chemical properties [6–8]. More generally, carbazole and its derivatives are important chemical intermediates, widely used in synthesis of pharmaceuticals, agrochemicals, dyes, pigments, and other organic compounds.

Carbazole (CZ) is produced commercially primarily from coal tar and crude oil; however, due to the increasing importance of CZ and its derivatives as valuable intermediates, synthetic production routes have been developed. These routes are based mainly around the liquid-phase dehydrogenation of 1,2,3,4-tetrahydrocarbazole (THCZ) (Fig. 1a) developed from Borsche carbazole synthesis [9]. A number of reducing agents [10] have been examined, including lead oxide as well as heterogeneous catalysts, such as Raney Ni [11] and supported Pd/C [12]. In the latter reactions, high temperatures in addition to low THCZ-to-catalyst ratios often are required.

These dehydrogenation reactions are usually performed under equilibrium conditions; therefore, high temperatures are required due to the endothermicity of the reaction. The yield of the dehydrogenation product also can be increased by removing the hydrogen thus formed. For batch liquid-phase dehydrogenations, high conversions are facilitated through the use of hydrogen acceptors, whereas a semibatch mode of operation can achieve the same outcome through the constant removal of hydrogen. In this regard, a range of hydrogen acceptors have been studied. For example, in the dehydrogenation of iminodibenzyl to iminostilbene, 2-nitrotoluene, *o*-dinitrotoluene, and diethylmaleate were compared; 2-nitrotoluene was found to provide the greatest conversion using a palladium-supported carbon catalyst [13,14]. The hydrogen acceptor-to-substrate molar ratio

* Corresponding author.
E-mail address: c.hardacre@qub.ac.uk (C. Hardacre).

0021-9517/$ – see front matter
doi:10.1016/j.jcat.2007.07.032

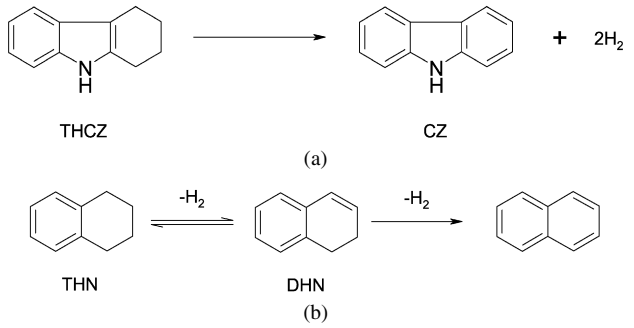

Fig. 1. Dehydrogenation reaction of (a) 1,2,3,4-tetrahydrocarbazole (THCZ) to form carbazole (CZ) and (b) tetrahydronaphthalene (THN) to naphthalene showing the formation of the intermediate dihydronaphthalene (DHN).

was found to be critical, with the highest conversion obtained at the stoichiometric ratio. Although a range of solvents has been studied, the high temperatures required limits the choices. Aromatic species, polyalcohols, and hydrogen acceptors have been compared, with polyalcohols found to provide the fastest reaction rates. Gaseous hydrogen acceptors also have been used in the dehydrogenation of benzylic and allylic alcohols to the corresponding carbonyl compounds over 10% Pd/C. Hayashi et al. [15] demonstrated that by using ethene, selective dehydrogenation of, for example, benzyl alcohol to benzaldehyde and steroidal alcohol to 19-nortestosterone could be achieved in high yields under mild conditions.

In this paper, we report the use of gaseous hydrogen acceptors for the dehydrogenation of THCZ that not only are potentially cheaper than the commonly used liquid acceptors, but also can be easily removed from the reaction mixture at the end of the reaction. We specify the detailed kinetics and mechanism of the dehydrogenation of THCZ over supported palladium catalysts in the presence of the hydrogen acceptor. This report is part of an ongoing study into this reaction, the detailed mechanism of which on palladium in the absence of a hydrogen acceptor was investigated previously using a combined experimental and density functional theory approach [16].

2. Experimental

2.1. Catalysts and materials

The catalysts used were Pd catalysts supported on either carbon or Al_2O_3 supplied by Johnson Matthey. All catalysts were characterised by BET N_2 isotherm and CO chemisorption. Table 1 summarises the catalyst characterisation data. For CO chemisorption, the catalyst samples were first reduced at 423 K in 5% H_2/Ar before being cooled to room temperature in He. This ensured that no hydride species existed during the experiment. Pulses of CO (2.38×10^{-6} mol) were then passed over the catalyst until saturation occurred. The metal dispersion was calculated using an assumed Pd:CO stoichiometry of 1:1. All solvents and reagents were used as received and were $\geqslant$99% purity, with the exception of carbazole, which was recrystallised from acetone before use. All average particle sizes are taken as the midpoint between the sieve sizes used (i.e., <75, 75–150, and 600–850 μm).

Table 1
Physical properties of the three catalysts employed in THCZ dehydrogenation reactions

Code	Catalyst	Support particle size (μm)	BET surface area ($m^2\ g^{-1}$)	Pd dispersion (%)
PdA-5	5% Pd/Al_2O_3	<50 μm	143	22.4
PdC-10	10% Pd/C	<50 μm	1358	16.5
PdAp-5[a]	5% Pd/Al_2O_3	3 mm[a]	82	6.4

[a] PdAp-5 was crushed and sieved to three particle size ranges of <75, 75–150, and 600–850 μm. Similar values for the Pd dispersion were measured for each fraction.

2.2. Semibatch reaction procedure

Semibatch reactions were undertaken in a glass three-necked, round-bottomed flask connected to a water-cooled condenser. The reaction temperature was controlled by an external silicone oil-heating bath, and the temperature in the reaction mixture was monitored by a thermocouple. Throughout the reaction, gas was purged directly through the reaction mixture. Typically, 0.4 g of 5 wt% supported Pd catalyst was charged to the reactor with 60 cm^3 mesitylene (Aldrich, $\geqslant$99%). N_2 was sparged through this mixture while stirring at 600 rpm with heating until the desired temperature was reached. At this point, corresponding to time zero, 23.4 mmol THCZ (Aldrich, 99%) dissolved in 20 cm^3 of mesitylene was added. Little change in rate was observed for stirring speeds above 600 rpm using this reactor, indicating that external mass transfer was not a significant issue. Samples of the reaction mixture were obtained at regular intervals and were diluted at a sample:diluent ratio of 1:3 before being analysed by high-pressure liquid chromatography (HPLC), using a chromatograph equipped with an Agilent Prep-C18 scalar column and an online UV detector. The diluent was a 50:50 v/v % mixture of EtOH and THF (Sigma–Aldrich, 99%). The purge gas could be varied among N_2, He, and H_2, with all the gases used being $\geqslant$99.99% purity (BOC). Reactions with tetrahydronaphthalene (THN) (Sigma–Aldrich, 99%) and dihydronaphthalene (DHN) (Sigma–Aldrich, 98%) were performed using the same reaction procedure and concentrations as for THCZ and were also analysed by HPLC.

2.3. Batch reactions procedure

Batch reactions were performed in a Premex 380 cm^3 stainless steel autoclave. Typically, 1.25 g of 5 wt% supported Pd catalyst was charged to the reactor with 240 cm^3 of mesitylene. This mixture was heated under stirring at 1400 rpm until the desired temperature was attained, as monitored by a thermocouple in the reaction mixture. Thereafter, 73.3 mmol THCZ dissolved in 10 cm^3 of mesitylene was added to the mixture, and the vessel was purged three times with N_2 or the hydrogen-accepting gas before being set to the desired reaction pressure. The stirrer was then set to 1400 rpm, corresponding to time zero. Samples were obtained at regular intervals and analysed as in the semibatch reactions.

For each reaction, the initial rate was taken as the gradient of the linear increase in carbazole formation over the 20% of reaction. For the variation of concentration with respect to time,

the error in the concentration of carbazole was estimated as $\pm 2.32 \times 10^{-3}$ M, corresponding to an error in reaction rate of 0.04×10^{-4} mol min^{-1} g_{cat}^{-1}.

2.4. Calculation details

The DFT calculations were performed using the SIESTA program. In this electronic structure code, the core electrons are replaced by norm-conserving pseudopotentials, and the valence orbitals are expanded in a nonorthogonal basis set of atom-centred orbitals. These orbitals are solutions of the isolated pseudo-atom but must disappear at a certain localisation radius. This produces an energy shift in their eigenvalues relative to the isolated pseudo-atom. In this work, an energy shift of 0.01 eV was used, which proved to be sufficiently small for the convergence of geometrical and energetic properties. The Hartree and exchange-correlation energies were calculated using a real space grid. The spacing of the grid points corresponds to an equivalent 150 Ry energy cutoff in the associated reciprocal space, which again was sufficient to ensure convergence of geometries and energies.

The exchange-correlation energy was determined using the generalised gradient approximation (GGA) functional proposed by Perdew, Burke and Ernzerhof (PBE) [17]. The GGA-PBE has proved to be a significant improvement over the local density approximation (LDA) for most chemical properties. The pseudopotentials were generated using the Troullier–Martins scheme, including a relativistic correction in the case of Pd. For all of the atoms, a double zeta with polarization quality basis set was used. The supercell approach (periodic boundary conditions) was taken to model the Pd surface; three layers of Pd atoms fixed at their bulk-truncated positions were used, and vacuum spacing of >10 Å was left between slabs. In previous work dealing with similar reactions over closely packed transition metal surfaces, the effect of increasing the number of metal layers and layer relaxation was thoroughly tested; for example, when 4 layers of metal atoms were used with the top layer relaxed, the reaction barriers were affected by <0.2 eV [18]. A $p(5 \times 5)$ unit cell was used in all of the calculations, and a Monkhorst–Pack mesh of $(2 \times 2 \times 1)$ was used in the k-point sampling. The transition states were determined by constraining the distance between the two reacting atoms while optimising the remaining degrees of freedom. The transition states were thus located when all of the forces on the atoms had reached a convergence criteria of 0.05 eV per Å and the total energy was maximum along the reaction coordinate but minimum with regard to all other degrees of freedom. Previous work has shown that the foregoing methods provide sufficient accuracy for the type of surface calculations considered in this work [16,19].

Although using DFT to examine the surface processes in liquid-phase reactions is valuable, it is important to recognise that the solute–solvent interaction will affect the adsorption energies. Any changes in adsorption energy will mainly affect the surface coverage, not the relative activation barriers, unless the solvent stabilises an intermediate state. Based on the reaction mechanisms examined herein, this seems unlikely; therefore, the use of "gas-phase" mechanistic arguments will indicate the relative importance of each of the surface processes.

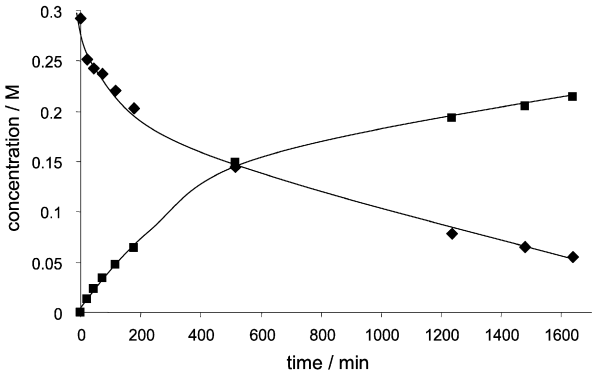

Fig. 2. Typical reaction profile for THCZ dehydrogenation reaction showing the formation of CZ (■) and the removal of THCZ (◆). Reaction conditions: 0.29 M THCZ, 5PdA catalyst, $T = 135$ °C, catalyst/THCZ mass ratio = 0.1.

3. Results

3.1. Semibatch mode

Fig. 2 shows a typical reaction profile for the dehydrogenation of THCZ to CZ at 408 K using 5PdA as the catalyst. CZ was the only product found. The reaction order was probed by varying the THCZ concentration between 0.029 and 0.584 M. No significant change in the initial reaction rate was observed, indicating that the reaction was zero order with respect to THCZ for both carbon- and alumina-supported catalysts. This is consistent with the reaction kinetics for the production of CZ, which increased approximately linearly up to an 8% conversion of THCZ. Thereafter, a positive order relationship was observed. To ensure that the reaction was not under external mass transfer control, the stirring speed and catalyst mass were varied for each catalyst tested. No change in the initial rate of reaction was observed at stirring speeds >600 rpm, and a first order relationship between reaction rate and catalyst mass was found at catalyst charges of 0.10–0.60 g. In the latter, a small deviation from linearity was found at low catalyst loadings, indicating the possible presence of catalyst inhibition. Due to the high adsorption strength of CZ, product poisoning was likely. To check this, a solution containing CZ was contacted with the catalyst before the THCZ was added to make up a final reaction mixture containing 0.015 M CZ and 0.292 M THCZ. Using this procedure, a significant drop in the initial reaction rate of THCZ conversion was noted; for example, using the 5PdA catalyst, a decrease from 1.04×10^{-4} to 7.82×10^{-5} mol min^{-1} g_{cat}^{-1} was observed at 135 °C, demonstrating the high degree of inhibition by CZ. The fact that similar behaviour was found for both alumina- and carbon-supported palladium indicates that the metal dominated the reaction mechanism and the support effect was limited.

3.2. Reaction solvent

Fig. 3 shows the effect of solvent on the reaction time profile. Similar reaction rates were found between aliphatic and

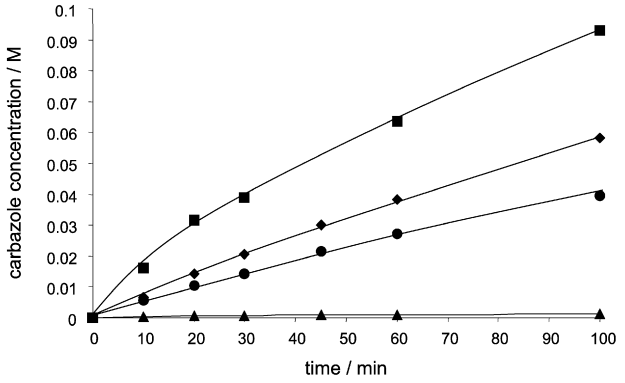

Fig. 3. CZ concentration with respect to time for THCZ dehydrogenation using mesitylene (◆), decane (●), diethylene glycol (▲) and diethyl maleate (■) as the reaction solvent. Reaction conditions: 0.29 M THCZ, 5PdA catalyst, $T = 135\,^{\circ}C$, catalyst/THCZ mass ratio = 0.1.

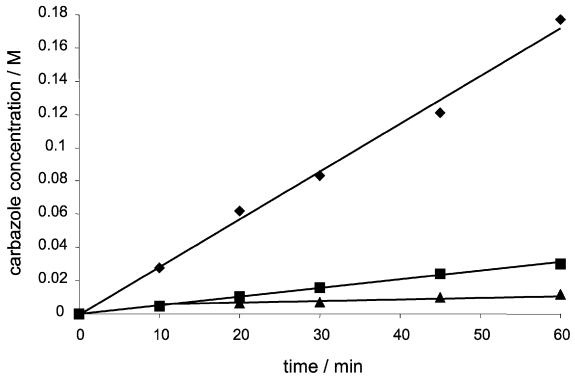

Fig. 4. CZ concentration with respect to time for THCZ reaction undertaken in semibatch mode under N_2 purge (■), batch mode with N_2 atmosphere (▲) and batch mode under initial pressure of 5 bar propene (◆). Reaction conditions: 0.29 M THCZ, 5PdA catalyst, $T = 135\,^{\circ}C$, catalyst/THCZ mass ratio = 0.1.

aromatic hydrocarbons. As found for the dehydrogenation of iminodibenzyl [18], the use of dimethyl maleate as a hydrogen-accepting solvent enhanced the rate of reaction. Using diethyl maleate, which contains a C=C functional group and can act as both a hydrogen acceptor and a solvent, resulted in a doubling of the initial rate of CZ formation compared with mesitylene. Although polyglycols have been shown to increase the rate of dehydrogenation, in this case no significant reaction was found using diethylene glycol. Commonly, polyglycols are used in conjunction with a hydrogen acceptor and, thus the role of the solvent in the reaction is not clear. Herein the glycol was detrimental to the reaction, probably through strong adsorption/chelation to the palladium, leading to blocking of the active surface sites.

The reaction rate in decane was slower than that in mesitylene. After 100 min, only 0.039 M CZ was formed in decane, compared with 0.059 M in mesitylene. This may be due to the difference in CZ solubility in the solvents. Approximating the solubility of CZ in mesitylene to that in benzene revealed that the solubility of CZ at 298 K was around 14 times greater in mesitylene than in decane [20]. This increased solvation by mesitylene would reduce the adsorption of the CZ on the palladium surface, reduce the effect of product inhibition, and consequently increase the rate of reaction.

3.3. Batch reactions

A purge gas reaction was used in all of the semibatch reactions. The assumption that the main purpose of the purge gas is to remove the dissolved hydrogen formed during the dehydrogenation reaction is supported by comparing the semibatch reaction with a reaction performed in a batch reactor under a N_2 atmosphere. Although over the first 10 min, the reaction showed the same reaction rate as for the semibatch reaction, the rate slowed significantly thereafter, with the yield after 100 min reduced by a factor of three (Fig. 4). Any effect of an oxidative dehydrogenation mechanism due to oxygen impurities in the nitrogen feed was eliminated in comparison with the semibatch reaction using a helium purge. The same reaction time profile was observed in both cases. The inhibiting effect of the dissolved hydrogen is further supported by the fact that when the nitrogen purge was switched to a hydrogen feed, the reaction ceased immediately. In this case, CZ was not back-hydrogenated to THCZ, but the presence of hydrogen did prevent further dehydrogenation through back-hydrogenation of the surface intermediates [16].

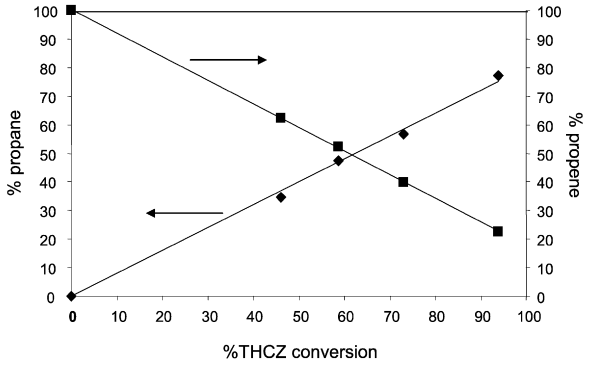

Fig. 5. Percentage propene (■) and propane (◆) in gas phase as a function of THCZ conversion during batch THCZ reaction with initial gas-phase pressure of 5 bar propene.

Importantly, when the reaction was performed under propene to act as a hydrogen acceptor, a significant increase in the rate was observed. At 408 K and under 5 bar propene, the batch reaction demonstrated a fivefold increase in the initial rate of reaction, as shown in Fig. 4. Interestingly, in the presence of propene, the reaction order with respect to THCZ changed from 0 to 0.5. To ascertain whether propane was formed in the reaction through the hydrogenation of propene, samples of the gas phase were obtained at regular intervals together with liquid samples. As THCZ conversion increased, the percentage of propane in the gas phase increased linearly with a concomitant decrease in propene (Fig. 5). The initial rates of reaction using 1 bar ethene or but-1-ene were compared with propene at 1 bar. But-1-ene and propene showed similar rates, 3.82×10^{-4} and 3.49×10^{-4} mol min^{-1} g_{cat}^{-1}, respectively, whereas ethene resulted in a reduced rate of 1.83×10^{-4} mol min^{-1} g_{cat}^{-1} (Fig. 6). The latter may be compared with the equivalent semibatch reaction with N_2 purge, which showed a rate approximately 1.8 times lower than that under ethene atmosphere.

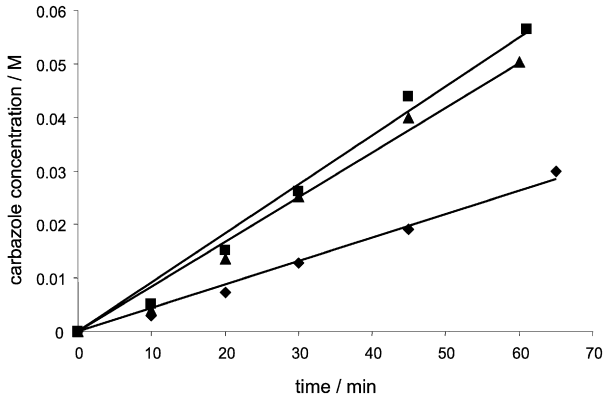

Fig. 6. CZ concentration with respect to reaction time for THCZ reaction undertaken in batch mode under 1 bar but-1-ene (▲), 1 bar propene (■) and 1 bar ethene (◆). Reaction conditions: 0.29 M THCZ, 5PdA catalyst, $T = 135\,^{\circ}C$, catalyst/THCZ mass ratio = 0.048.

3.4. Molecular adsorption and mechanism of propene promotion

The mechanism of the nonpropene-promoted reaction has been studied in detail in our laboratory [16]; our findings indicate that the first hydrogen abstraction is the rate-limiting step, with an activation barrier of 0.87–0.95 eV. To examine the role of propene in promoting the reaction rate, we studied two mechanisms: (1) propene acting as a cofactor and lowering the activation barrier for THCZ dehydrogenation and (2) adsorption and hydrogenation of propene by surface-adsorbed hydrogen.

We investigated the adsorption geometries and adsorption energies of THCZ and CZ over Pd(111), and also investigated THCZ adsorption energy in the presence and absence of propene over Pd(111). Without propene, THCZ adsorbed flat on the Pd surface, with an adsorption energy of −1.49 eV, and CZ also adsorbed flat on the surface with a slightly stronger interaction, giving an adsorption energy of −1.59 eV. Without propene, the adsorbed THCZ molecule had three hydrogen atoms near the Pd surface available for dehydrogenation at 2.11–2.91 Å from the surface. On adsorption of a propene molecule, which had a calculated adsorption energy of −0.96 eV, the THCZ adsorption geometry did not change. Therefore, it is unlikely that the propene modified the adsorption mode to increase the THCZ dehydrogenation rate by, for example, forcing the reactive hydrogens closer to the Pd surface. Propene also can form an activated complex with the THCZ and directly accept a hydrogen atom from THCZ without the hydrogen dissociating and chemisorbing on the Pd surface. The complex formed from surface-adsorbed propene had an activation barrier of 2.02 eV, much higher than the calculated THCZ dehydrogenation barrier in the absence of propene of 0.87–0.95 eV [16]. The high activation energy is due to the energy required to break a Pd–C bond during this mechanism, as shown in Fig. 7. Complex formation via gas-phase propene and subsequent hydrogen abstraction is more favourable than the surface-mediated process with an activation barrier of 1.18 eV; however, this pathway has a slightly higher barrier compared with that found for the nonpropene-promoted route. More importantly, this mechanism

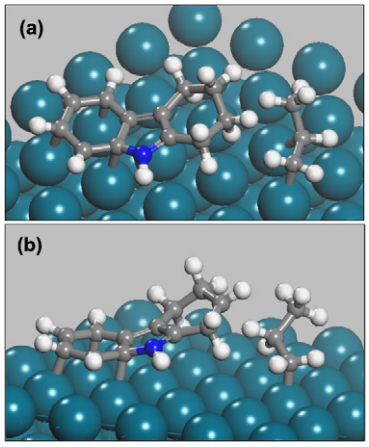

Fig. 7. Formation of the THCZ-propene activated complex. (a) The co-adsorption of THCZ and propene on Pd(111) prior to transition state formation with the propene forming two C–Pd bonds with the surface. (b) The activated complex formed between propene and THCZ; transition state formation requires cleavage of one Pd–C bond and the abstraction of a THCZ H atom by propene.

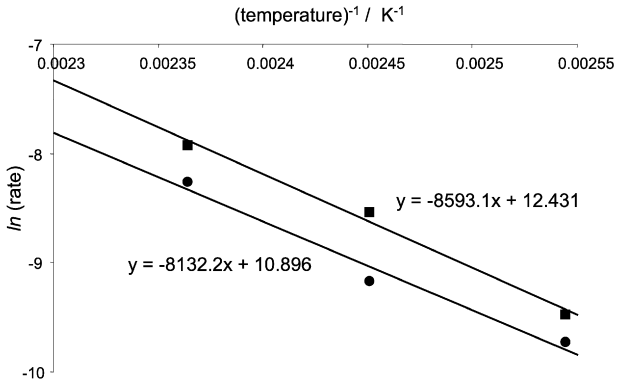

Fig. 8. Arrhenius plot for dehydrogenation of THCZ over PdA-5 without propene (●) and PdA-5 with propene (■).

would cause a significant decrease in the entropy of the transition state and thus is unfavored.

Comparing the activation barrier for propene hydrogenation from surface-adsorbed hydrogen atoms with the back-hydrogenation of the possible THCZ intermediates shows similar values at 0.85 and 0.50–1.23 eV, respectively. This similarity suggests that propene hydrogenation to propane can compete with the back-hydrogenation of the intermediate to reform THCZ and shift the THCZ dehydrogenation equilibrium toward the CZ by removing the surface-adsorbed hydrogen. In this mechanism, the observed increase in rate was not due to a change in activation barrier, but rather to an increase in the surface coverage of the intermediate. That the dehydrogenation activation barrier was unaltered in the presence of propene is in good agreement with the experimental determination of apparent activation barriers in the absence and presence of propene. Without propene, PdA-5 showed an apparent activation energy of 67 kJ mol^{-1}, compared with 71 kJ mol^{-1} in the presence of propene (Fig. 8).

Interestingly, despite the much weaker adsorption energy of propene (−0.96 eV) on a clean Pd(111) surface compared with THCZ (−1.49 eV), the propene must adsorb and compete with

the substrate, reducing its surface coverage and leading to the experimentally observed change in reaction order with respect to THCZ from 0 to 0.5. This finding is also supported by the fact that the rate is found to be zero order with respect to the propene over the pressure range of 1–9 bar. A comparison of the solubility of propene and THCZ in mesitylene shows that the relative adsorption energies from the gas-phase DFT calculations will be significantly altered by the presence of the solvent. Assuming that the gas solubility in mesitylene can be approximated to that found in toluene, the maximum propene solubility at 25 °C and 5 bar is around 100 times less than the THCZ concentration used [21]. Furthermore, the solubility of propene decreases exponentially with temperature, unlike that of THCZ, which increases with temperature, so that the difference will be even more pronounced at the temperature of the reaction. Therefore, the net effect of the solvation is to reduce the adsorption energy of the THCZ more than the propene thus increasing the relative surface coverage of propene over THCZ compared with that predicted from the gas-phase model. The effect of differing adsorption strengths arising from solvation effects has been used to perform stereoselective and competitive reactions [22,23].

The relative rates of dehydrogenation in the presence of ethene, propene, and but-1-ene also may be explained by their respective gas solubilities. Once again, assuming that the gas solubility in mesitylene can be approximated to that found in toluene, Atiqullah et al. have shown that the solubility of propene is approximately five times higher than that of ethene at 60 °C [21]. Given that our calculated adsorption energies of ethene, propene, and but-1-ene were similar at −1.09, −0.96, and −0.96 eV, respectively, the increased solubility led to a higher surface coverage of propene and but-1-ene compared with that of ethene and thus a higher rate.

4. Discussion

CZ clearly acts as a catalyst inhibitor for the THCZ dehydrogenation reaction; however, the DFT calculations showed that CZ had only a 0.1-eV stronger adsorption energy in the gas phase. As suggested for the difference in catalyst activity with decane and mesitylene solvents and the occurrence of competitive adsorption between THCZ and propene, solvent–adsorbate interactions also affect the adsorption strength of the reactant and product. Based on solubility studies, CZ had a solubility of ∼0.08 M in mesitylene at 80 °C, whereas that of THCZ was approximately 40 times greater. The greater solubility and lower adsorption energy of THCZ compared with those of CZ explains why the reaction was product-inhibited.

The importance of hydrogen removal is clearly demonstrated by the rate increases observed when using a purge gas or hydrogen acceptor. In both cases, it has been suggested that this removal hinders the back-reaction of the product; that is, at least one step in the process is reversible, and thus removing the hydrogen shifts the equilibrium position in favour of the desired product. It was observed that when the N_2 purge gas was replaced by a hydrogen stream, the reaction ceased; however, no hydrogenation of the CZ product was observed, indicating that it is the reversibility of the intermediates on the surface (as no bulk intermediates were observed) that controls this equilibrium. It was not possible to prove this theory using the THCZ reaction, because these intermediates are not commercially available and could not be isolated during a reaction. However, for the similar dehydrogenation reaction of tetrahydronaphthalene (THN) to naphthalene (Fig. 1b), dehydrogenation of the intermediate dihydronaphthalene (DHN) can be studied. The dehydrogenation of THN was comparable to that of CZ when carried out at 135 °C; however, the DHN dehydrogenation reaction was significantly faster and was performed at 70 °C, indicating that the conversion of THN to DHN was the rate-determining step in the overall conversion to naphthalene. As was found in the dehydrogenation of THCZ to CZ, a rate enhancement for THN dehydrogenation was observed when propene was used as a hydrogen acceptor (Fig. 9). In this case, a sixfold increase in rate was found.

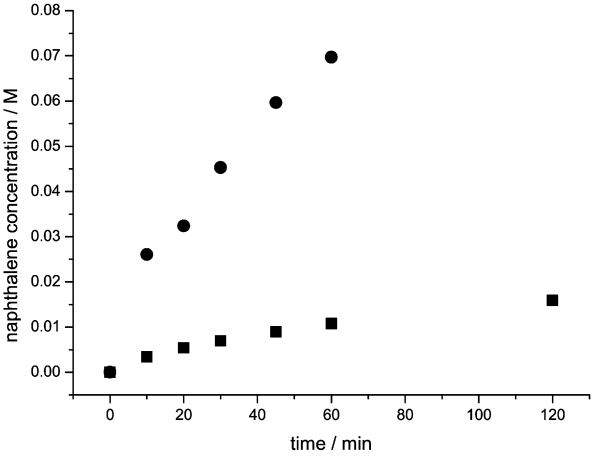

Fig. 9. Naphthalene concentration with respect to time for THN reaction undertaken in semibatch mode under N_2 purge (■) and under initial pressure of 1 bar propene (●). Reaction conditions: 0.29 M DHN, 5PdA catalyst, $T = 135$ °C, catalyst/THN mass ratio = 0.16.

Interestingly, when dehydrogenation of the intermediate DHN was studied under N_2 purge gas conditions, the back-hydrogenated THN product was observed in equimolar concentrations to the desired naphthalene product. This result suggests that under these conditions, the rate of back-hydrogenation was faster than the combined rate of DHN dehydrogenation and hydrogen removal from the surface (Fig. 10), and that all of the hydrogen produced was consumed immediately. However, under a propene atmosphere, the addition of propene competed with the hydrogenation of DHN and decreased the rate of THN formation and increased the naphthalene selectivity.

Fig. 4 shows that the initial rates for both the purged and unpurged systems were similar and deviated only after several minutes, suggesting that some degree of hydrogen storage existed within the catalyst. Whereas this storage effect would be affected only slightly by bulk mixing (i.e., mixing rates or purge gas flow rate), it would be a stronger function of particle size. When PdAp-5 was crushed and sieved to give three different particle size ranges, the resulting reaction rates followed a linear relationship with the ln (average particle diameter), with the average particle size taken as the midpoint within the sieved range. Smaller particles gave the highest rate, which is symp-

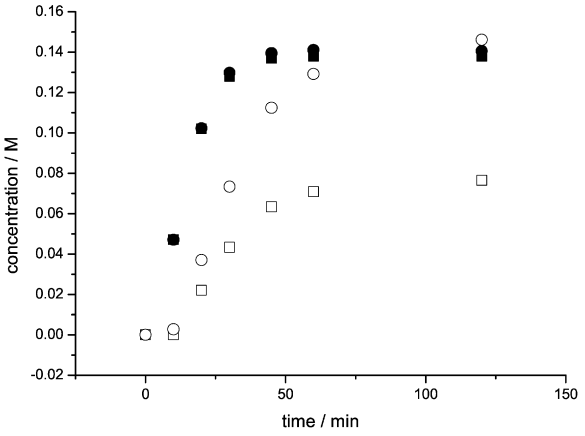

Fig. 10. Concentration of THN (squares) and naphthalene (circles) with respect to time for DHN reaction undertaken in semibatch mode using a N_2 purge (closed symbols), and under initial pressure of 5.5 bar propene (open symbols). Reaction conditions: 0.29 M DHN, 5PdA catalyst, $T = 70\,^{\circ}C$, catalyst/DHN mass ratio = 0.16.

tomatic of reaction under an internal (pore) diffusion limitation. Such effects often are observed in hydrogenations where hydrogen diffusion into the catalyst pores can be rate-limiting [24]; for example, in the hydrogenation of 3-methyl-1-pentyn-3-ol, a relatively fast reaction, H_2 internal mass transfer is rate-limiting for catalyst particles above an average threshold diameter of around 20 μm [25]. Here such effects would have been observed had either THCZ diffusion into or hydrogen diffusion from the pore been limiting. For the case of THCZ diffusion, initial calculations using the Weisz–Prater criterion [26] indicate that for each catalyst tested, THCZ diffusion was not limiting. Thus, the particle size effect is considered to result from the hold-up of the hydrogen within the catalyst pores. The larger particles then lead to a longer hydrogen residence time and consequently an unfavourable equilibrium, which in turn decreases the overall rate of CZ formation. This result could have significance in many dehydrogenation reactions, especially those that use catalysts not in powdered form. Moreover, the pore volume could play a vital role, highlighting the importance of catalyst design.

Whereas the liquid-phase acceptors showed a marked increase in reaction rate, the gas-phase acceptors are considered an economically viable alternative for such high-temperature reactions; for example, bulk costs for nitrotoluene are approximately 1.4 times that of propene. In addition, separation of the transfer hydrogenation product is facile in the case of propene but requires an additional distillation step when using liquid-based acceptors. However, the use of gas-phase hydrogen acceptors necessitates the use of closed pressurised reactors, which generally are more costly than atmospheric vessels operating under reflux.

5. Conclusion

A hydrogen acceptor has proved to increase the reaction rate in this case. Furthermore, there is potential for increasing the rate further by increasing the reaction temperature above the boiling point of the solvent, as the process can be performed in a batch mode of operation under pressure. With an activation energy of $\sim$70 kJ mol^{-1}, small increases in temperature could yield significantly faster reaction rates. Comparison of rates at equal temperature demonstrated that the incorporation of propene was equivalent to raising the reaction temperature by 35 °C. The use of a hydrogen-accepting gas like propene to remove hydrogen produced in the reaction, thus preventing hydrogenation of the intermediates, represents a more economic alternative to the use of liquid hydrogen acceptors. Not only is the propene less expensive than, for example, nitrotoluene and diethyl maleate, but the workup issues are simpler, with both the propene and propane products separating easily from the solution as gases.

Acknowledgment

Funding was provided by the EPSRC under the CARMAC project.

References

[1] V. Barbieri, M.G. Ferlin, Tetrahedron Lett. 47 (2006) 8289.
[2] D. Pelaprat, R. Oberlin, I. Le Guen, B.-P. Roques, J.B. Le Pecq, J. Med. Chem. 23 (1980) 1330.
[3] H.-J. Knölker, Top. Curr. Chem. 244 (2005) 115.
[4] Z. Liu, R.C. Larock, Tetrahedron 63 (2007) 347.
[5] T. Kitawaki, Y. Hayashi, A. Ueno, N. Chida, Tetrahedron 62 (2006) 6792.
[6] L. Feng, C. Zhang, H. Bie, Z. Chen, Dyes Pigm. 64 (2005) 31.
[7] L. Liu, W.-Y. Wong, J.-X. Shi, K.-W. Cheah, T.-H. Lee, L.M. Leung, J. Organomet. Chem. 691 (2006) 4028.
[8] S.K. Pisharady, C.S. Menon, C.S. Kumar, T.G. Gopinathan, Mater. Chem. Phys. 100 (2006) 147.
[9] W. Borsche, A. Witte, W. Bothe, Ann. Chem. 359 (1908) 49.
[10] R. Robinson, Chem. Rev. 63 (1963) 373.
[11] Y. Majin, C. Zhongjun, L. Dadong, Dying Ind. 36 (1998) 21.
[12] E.C. Horning, M.G. Horning, G.N. Walker, J. Am. Chem. Soc. 70 (1948) 3935.
[13] I. Köhegyi, V. Galamb, Heterocycles 40 (1995) 109.
[14] V. Galamb, F. Joó, I. Köhegyi, J. Chem. Res. (1995) 216.
[15] (a) M. Hayashi, K. Yamada, S. Nakayama, Synthesis (1999) 1869;
(b) M. Hayashi, K. Yamada, S. Nakayama, J. Chem. Soc. Perkin Trans. 1 (2000) 1501;
(c) M. Hayashi, K. Yamada, S. Nakayama, H. Hayashi, S. Yamazaki, Green Chem. 2 (2000) 257.
[16] P. Crawford, R. Burch, C. Hardacre, K.T. Hindle, P. Hu, B. Kalirai, D.W. Rooney, J. Phys. Chem. C 111 (2007) 6434.
[17] J.P. Perdew, K. Burke, M. Ernzerhof, Phys. Rev. Lett. 77 (1996) 3865.
[18] A. Michaelides, P. Hu, J. Chem. Phys. 114 (2001) 5792.
[19] L.M. Liu, B. McAllister, H.Q. Ye, P. Hu, J. Am. Chem. Soc. 128 (2006) 4017.
[20] P. Ruelle, E. Sarraf, U.W. Kesselring, Int. J. Pharm. 104 (1994) 125.
[21] M. Atiqullah, H. Hammawa, H. Hamid, Eur. Polym. J. 34 (10) (1998) 1511.
[22] L. Gilbert, C. Mercier, in: M. Guisnet, J. Barbier, J. Barrault, G. Bouchoulo, D. Duprez, G. Pérot, C. Montassier (Eds.), Heterogeneous Catalysis and Fine Chemicals, vol. III, Elsevier, Amsterdam, 1993, p. 51.
[23] U.K. Singh, M.A. Vannice, Appl. Catal. A 213 (2001) 1.
[24] K.T. Hindle, S.D. Jackson, D. Stirling, G. Webb, J. Catal. 241 (2006) 417.
[25] T.A. Nijhuis, G. van Koten, F. Kapteijn, J.A. Moulijn, Catal. Today. 79–80 (2003) 315.
[26] P.B. Weisz, C.D. Prater, Adv. Catal. 6 (1954) 144.